

Electronic Supplementary Information (ESI) for

**Controllable Asymmetrical/Symmetrical Coating Strategy
for Architecture Mesoporous Organosilica Nanostructures**

Xue Wang, Yapeng He, Chong Liu, Yunling Liu, Zhen-An Qiao* and Qisheng Huo

*State Key Laboratory of Inorganic Synthesis and Preparative Chemistry, College of Chemistry,
Jilin University, Changchun 130012, People's Republic of China.*

**E-mail: qiaozhenan@jlu.edu.cn*

Fax: +86-431-85168624; Tel: +86-431-85168602

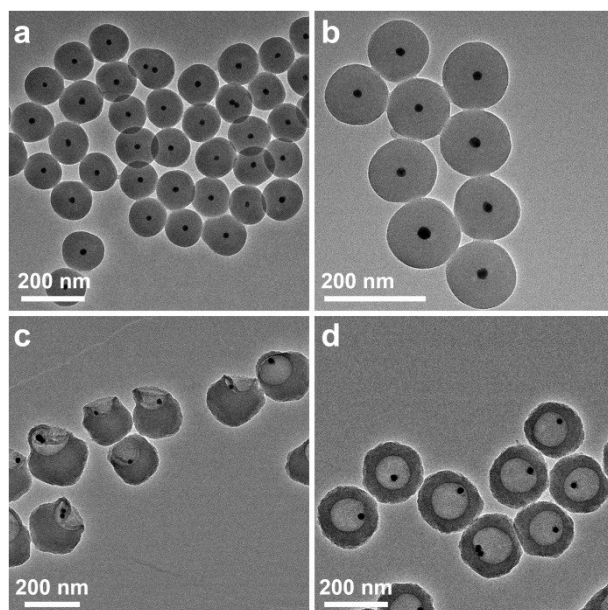


Figure S1. TEM images of (a), (b) core-shell Au@SiO₂, (c) Janus Au&PMO, (d) yolk-shell Au@PMO nanoparticles.

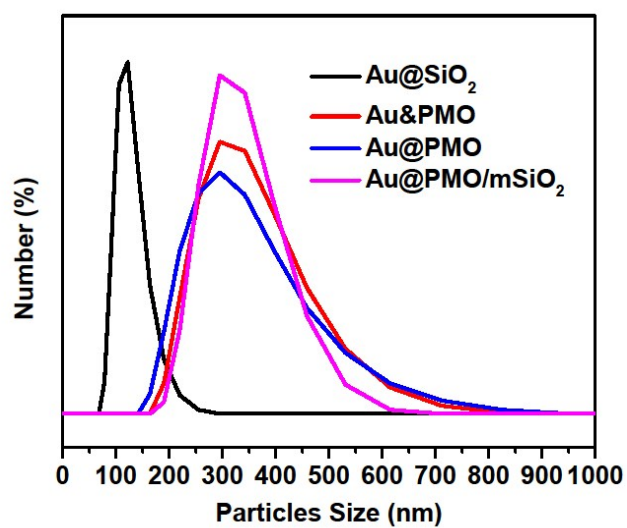


Figure S2. Hydrodynamic diameters of Au@SiO₂, Au&PMO, Au@PMO and Au@PMO/mSiO₂ nanoparticles.

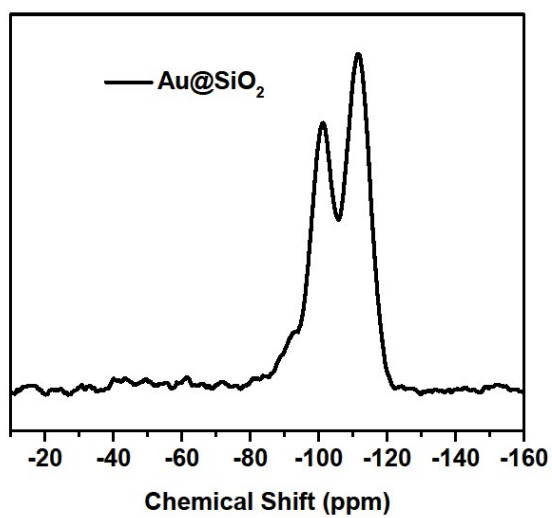


Figure S3. ^{29}Si MAS NMR spectra of $\text{Au}@SiO_2$ nanoparticles.

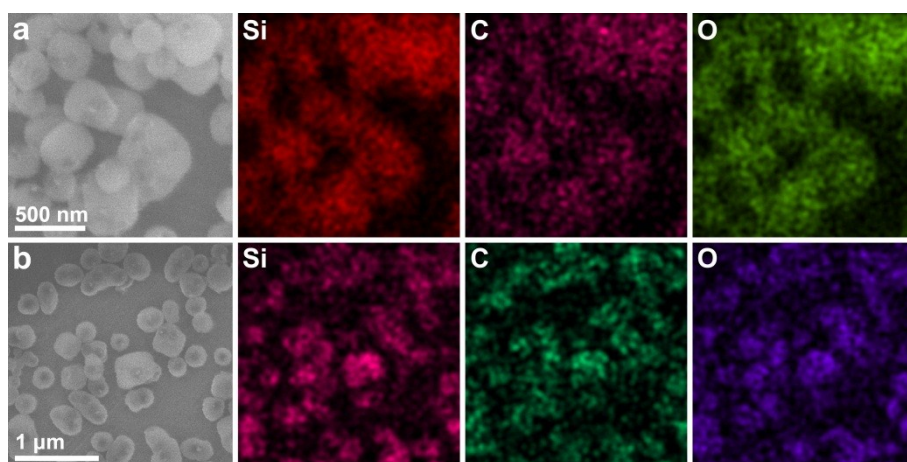


Figure S4. The SEM images and elemental mapping of (a) Au&PMO and (b) Au@PMO nanoparticles.

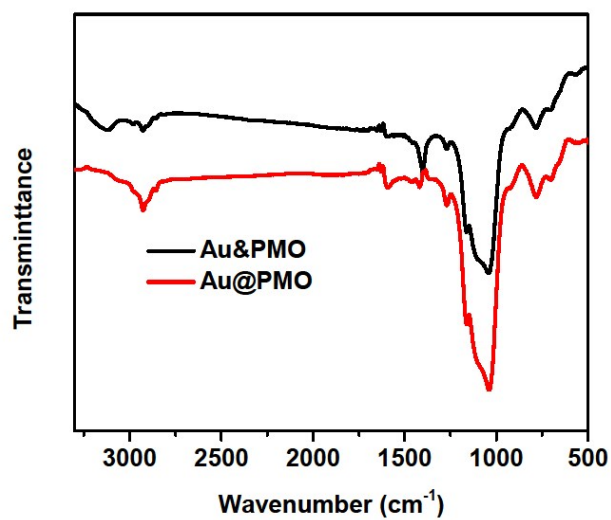


Figure S5. FTIR spectra of Au&PMO and Au@PMO nanoparticles.

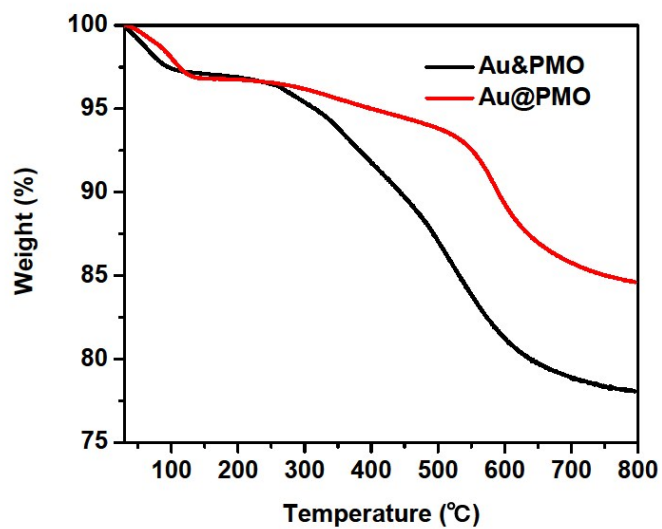


Figure S6. TG curves of Au&PMO and Au@PMO nanoparticles.

Table S1. Physicochemical properties of Au&PMO, Au@PMO and Au@PMO/mSiO₂ nanoparticles.

Sample	BET Surface Area (m ² g ⁻¹)	Pore Diameter (nm)	Pore Volume (cm ³ g ⁻¹)
Au&PMO	964	2.2	0.99
Au@PMO	884	2.1	0.97
Au@PMO/mSiO ₂	429	2.1, 6.1	0.60

Pore Diameter is BJH pore diameter calculated by the adsorption branches of the nitrogen sorption isotherms.

Pore Volume is the total pore volume determined at the relative pressure P/P₀ of 0.99.

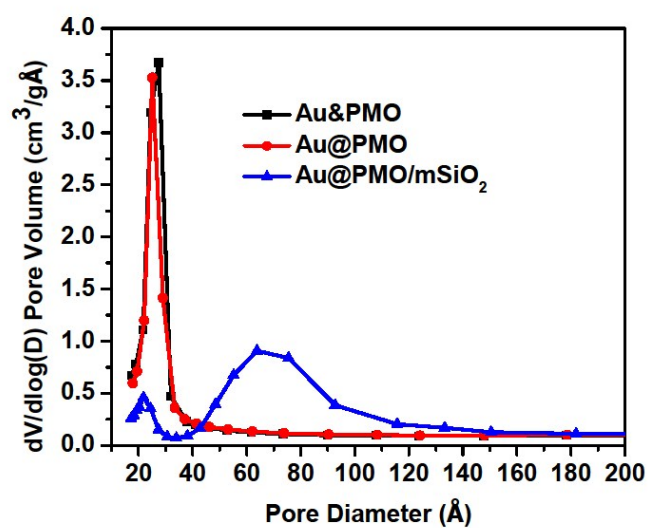


Figure S7. Pore size distribution curves of Au&PMO, Au@PMO and Au@PMO/mSiO₂ nanoparticles.

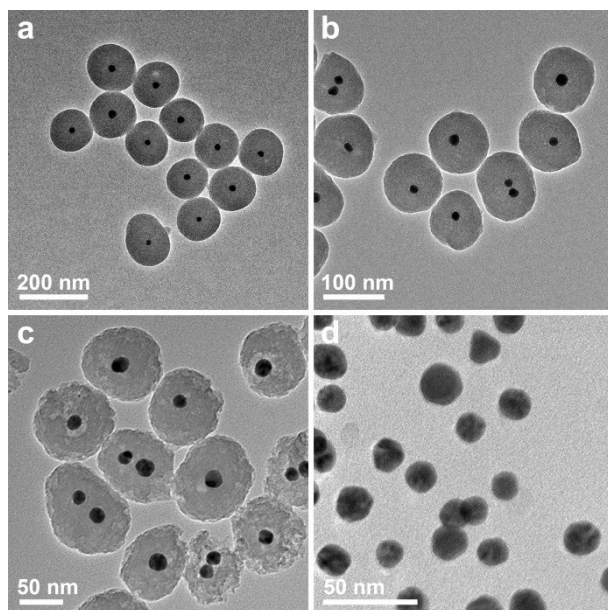
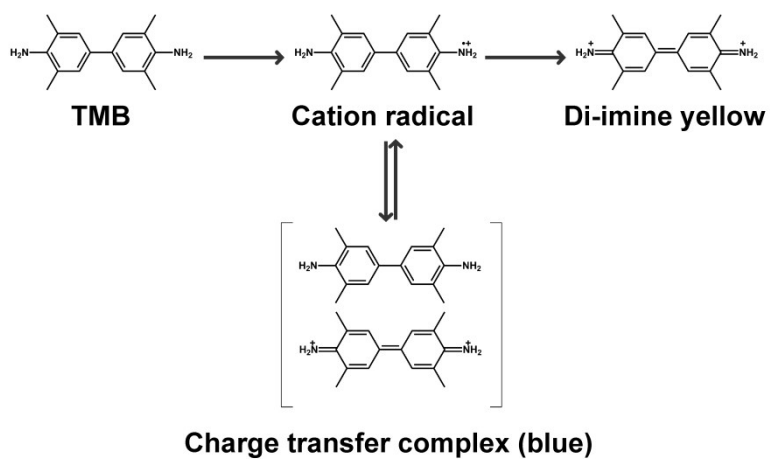


Figure S8. TEM images of Au@SiO₂ nanospheres etched by ammonia at different reaction time: (a) 0 h, (b) 0.5 h, (c) 1 h, (d) 3 h.



Scheme S1. Chemical structure of TMB, its oxidation products and reaction scheme of TMB oxidation.

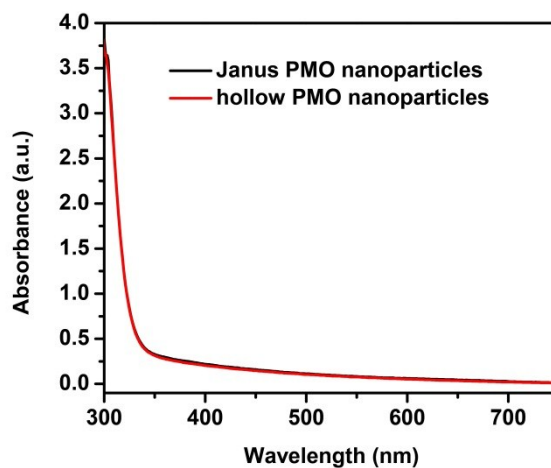


Figure S9. UV-vis absorbance changes at catalyzed oxidation of TMB by using Janus or hollow PMO nanoparticles without Au cores as catalysts.

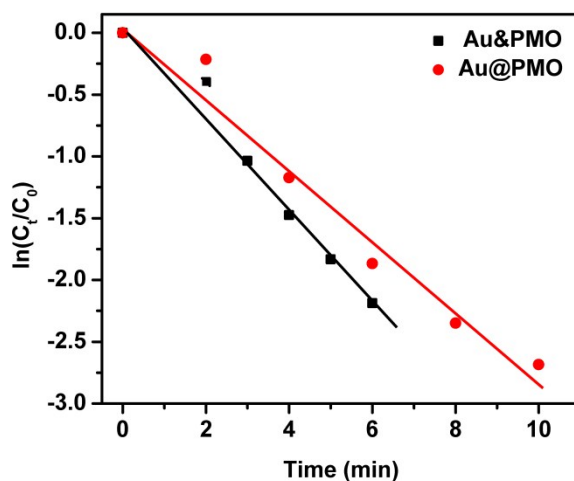


Figure S10. Kinetic analysis of the catalytic reactions and plot of $\ln(C_t/C_0)$ versus time for 4-nitrophenol. The ratio of C_t and C_0 , where C_t and C_0 are 4-nitrophenol concentrations at time t and 0, respectively, is measured from the relative intensity of the respective absorbance, A_t/A_0 . The linear relations of $\ln(C_t/C_0)$ versus time indicate that the reaction follows first-order kinetics.

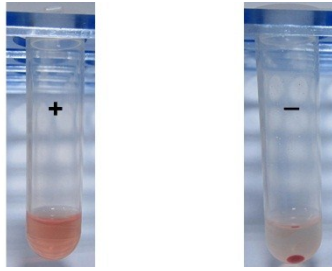


Figure S11. Photographs of hemolysis of RBCs incubated with water and physiological saline; water (+) and physiological saline (-) were used as positive and negative control, respectively.

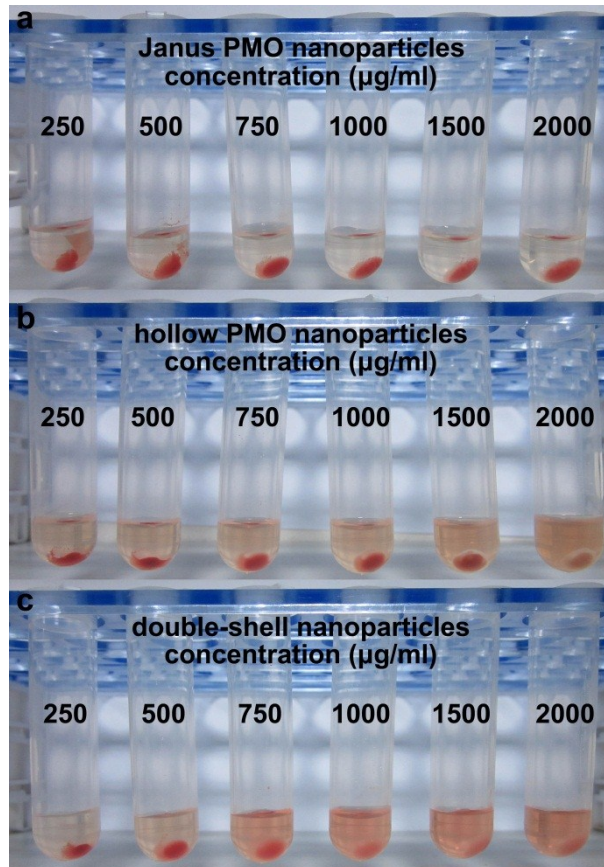


Figure S12. Photographs of hemolysis of RBCs incubated with three types of nanoparticles; the presence of red hemoglobin in the supernatant indicates damaged RBCs.

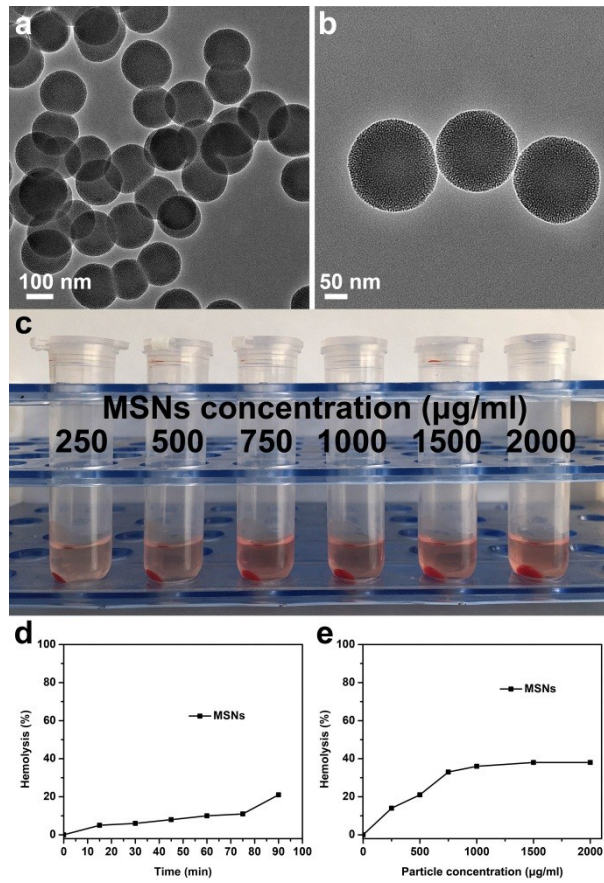


Figure S13. (a), (b) TEM images of MSNs; (c) photographs of hemolysis of RBCs incubated with MSNs (the presence of red hemoglobin in the supernatant indicates damaged RBCs); hemolysis percentage of RBCs incubated with MSNs (d) at a concentration of 500 µg/ml for different times; (e) at different concentration ranging from 250 to 2000 µg/ml.